Supporting Information

Ortho-Substituent Induced Triradical-Containing Tetranuclear Oxo–Vanadium(IV) Cluster Formation via Ligand C–N Bond Breaking and C–O Bond Making

Samir Ghorai and Chandan Mukherjee*

***Corresponding address:**

Dr. Chandan Mukherjee, Department of Chemistry, Indian Institute of Technology, Guwahati, 781039, Assam, India

Email: cmukherjee@iitg.ernet.in

Tel. +91-361-258-2327

Fax: +91-361-258-2349

2 = Vanadium complex formed with ligand H_2Sami^{OMe}

Materials:

All the chemicals and solvents were obtained from commercial sources and were used as supplied, unless noted otherwise. 3,5-di-*tert*-butylcatechol, and 2-aminobenzonitrile were purchased from Sigma-Aldrich. Solvents were obtained from Merck (India).

Physical Method:

X-ray crystallographic data were collected using a Bruker SMART APEX-II CCD diffractometer, equipped with a fine focus 1.75 kW sealed tube Mo–Kα radiation (λ = 0.71073 Å) at 296(2) K, with increasing w (width of 0.3° per frame) at a scan speed of 3 s/frame. Structures were solved by direct methods using SHELXS-97 and refined with full-matrix least squares on F^2 using SHELXL-97. All then non-hydrogen atoms were refined anisotropically.

IR spectra were recorded on Perkin Elmer Instrument at normal temperature making KBr pellet grinding the sample with KBr (IR Grade). UV-vis spectra were recorded on Perkin Elmer, Lamda 750, UV/VIS/NIR spectrometer preparing a known concentration of the samples in HPLC Grade CH_2Cl_2 at room temperature using cuvette of 1 cm width. EPR spectra were measured on X-Band Microwave Unit, JES-FA200 ESR spectrometer. Variable–temperature magnetic measurements have been performed using VSM (Physics Department, Indian Institute of Science, Bangalore, India)

Experimental Section:

Synthesis of $C_{21}H_{26}N_2O$, H_2Sami^{CN}. To a suspension of 3,5–di–*tert*–butylcatechol (2.22 g, 10 mmol) and 2–aminobenzonitrile (1.18 g , 10 mmol) in hexane (40 mL), 0.05 mL of triethylamine was added and the suspension was refluxed for two days. During the time a homogeneous yellow colour solution appeared that turned to red upon stirring at room temperature (30 °C) under air for four days. After that, the reaction mixture was kept at 4 °C for overnight. This caused precipitation of unreacted 2–aminobenzonitrile. The solution was decanted and was kept for precipitation. The precipitate was then recrystallized thrice from a 5:1 CH_2Cl_2:EtOH solvent mixture. A colourless crystalline solid appeared. Washed with EtOH and then dried under air. Yield: 2.320 g, 72%. FTIR (KBr pellet cm^{-1}): 3421, 3354, 2950, 2904, 2864, 2221, 1600, 1577, 1504, 1481, 1458, 1444, 1419, 1360, 1318, 1308, 1290, 1217, 1197, 1163, 976, 759. ^{1}H NMR ($CDCl_3$, 399.85 MHz): δ 1.27 (s, 9H), 1.44 (s, 9H), 5.83 (s, N–H), 6.00 (s, 1H), 6.5 (d, J = 8.8 Hz, 1H), 6.85 (t, J = 7.6 Hz, 1H), 7.01 (s, 1H), 7.28 (s, 1H), 7.34 (t, J = 8 Hz, 1H), 7.50 (d, J = 7.6 Hz, 1H). ^{13}C NMR ($CDCl_3$, 100.55 MHz): δ 29.71, 31.76, 34.61, 35.30, 98.00, 114.13, 117.68, 119.41, 122.21, 123.47, 125.36, 132.83, 134.58, 136.34, 143.05, 149.43 and 149.89. ESI–MS(+) *m/z* for [$C_{21}H_{26}N_2O$ + H]: calcd, 323.21; found, 323.55. UV-vis (CH_2Cl_2) λ_{max}, nm (ε, $M^{-1}cm^{-1}$): 396 (450), 320 (4750), 283 (4850), 248 (8800). Anal. Calcd for $C_{21}H_{26}N_2O$: C, 78.22; H, 8.12; N, 8.69. Found: C, 78.53; H, 8.34; N, 9.08.

Synthesis of [($C_{60}H_{102}N_1S_1O_{17}V_4$)•$CH_3CN$], 1•1$CH_3CN$. To a methanolic solution (30 mL) of H_2Sami^{CN} (0.497 g, 1.54 mmol), $VO(SO_4)$•$5H_2O$ (0.394 g, 1.56 mmol) and triethyl amine (0.2 mL) were added and the resulting solution was refluxed for two hours. After that, the solution was stirred for another two hours at room temperature and then filtered and the filtrate was kept for slow evaporation. This caused precipitation of blue microcrystalline solid. Filtered and the solid residue was thoroughly washed with methanol, and then, dried under vacuum. Yield: 0.265 g.

To 15:5:5 CH_2Cl_2:CH_3CN:MeOH solution of the blue solid (0.050 g), tetrabutylammonium perchlorate (0.060 g, 0.175 mmol) was added. Slow evaporation of the solution caused precipitation of block shaped blue crystalline solid suitable for single crystal X-ray diffraction study. Yield: 0.048 g, 47% [with respect to $VO(SO_4)$•$5H_2O$]. FTIR (KBr pellet, cm^{-1}): 2961, 2913, 2873, 1584, 1459, 1438, 1272, 1236, 1102, 1046, 1015, 998, 982, 689, 657, 627, 587. ESI–MS (-ve) *m/z* for $[C_{44}H_{66}O_{17}SV_4]^-$: calcd, 1102.18; found, 1101.92, ESI–MS (+ve) *m/z* for $[C_{16}H_{36}N]^+$: calcd, 242.28; found, 242.25. Anal. calcd for $C_{44}H_{66}O_{17}SV_4$•1CH_3CN•1H_2O: C, 53.03; H, 7.68; N, 2.0. Found: C, 53.01; H, 7.75; N, 2.36.

Synthesis of [$C_{21}H_{29}NO_2$], H_2Sami^{OMe}. A mixture of 3,5–di–*tert*–butylcatechol (2.22 g, 10 mmol), *o*–anisidine (1.23 g, 10 mmol), and Et_3N (0.1 mL) in hexane (35 mL) was refluxed for 24 h. After that, the resulting red solution was stirred at room temperature (30 °C) for another 24 h. The solution was then kept at 4 °C for overnight. A white precipitate appeared, which was filtered and recrystallized from a 5:1 CH_2Cl_2:MeOH solvent mixture. Yield: 2.025 g, 62 %. FTIR (KBr pellet, cm^{-1}): 3482, 3395, 3005, 2957, 2901, 2868, 1595, 1511, 1487, 1451, 1425, 1391, 1360, 1331, 1304, 1249, 1220, 1200, 1177, 1151, 1119, 1109, 1045, 1020, 974, 877, 824, 754, 742, 651, 575. ESI–MS (+) *m/z* for [$C_{21}H_{29}NO_2$ + H]: calcd, 328.47; Found, 328.59. ^{1}H NMR ($CDCl_3$, 399.85 MHz): δ 1.26 (s, 9H), 1.45 (s, 9H), 3.93 (s, 3H), 5.56 (s, N–H), 6.44 (m, 2H), 6.76–6.82 (m, 2H), 6.86–6.88 (m, 1H), 7.01 (d, *J* = 1.2 Hz, 1H), 7.21 (m, *J* = 2.2 Hz, 1H) ppm. ^{13}C NMR ($CDCl_3$, 100.55 MHz): δ 29.76, 31.84, 34.57, 35.20, 55.71, 110.12, 113.56, 119.28, 121.45, 121.81, 121.95, 127.81, 135.31, 136.69, 142.24, 147.77, 149.87 ppm.

Synthesis of [$C_{21}H_{29}NO$], H_2Sami^{Me}. This compound was synthesised in a manner analogous to that for H_2Sami^{OMe}. FTIR (KBr pellet, cm^{-1}): 3409, 3369, 3030, 2961, 2901, 2867, 1607, 1597, 1586, 1498, 1480, 1419, 1391, 1361, 1308, 1261, 1253, 1238, 1226, 1202, 1158, 1116, 1109, 1050, 972, 882, 823, 808, 795, 747, 712. ESI–MS (+) *m/z* for [$C_{21}H_{29}NO$ + H]: calcd, 312.47; Found, 312.58. ^{1}H NMR ($CDCl_3$, 399.85 MHz): δ 1.27 (s, 9H), 1.44 (s, 9H), 2.32 (s, 3H), 4.88 (s, N–H), 6.36 (s, O–H), 6.42 (d, *J* = 8 Hz, 1H), 6.80 (t, *J* = 7 Hz, 1H), 6.99 (d, *J* = 2 Hz, 1H), 7.04 (t, *J* = 7.2 Hz, 1H), 7.14 (d, *J* = 7.2 Hz, 1H), 7.23 (t, *J* = 2 Hz, 1H) ppm.

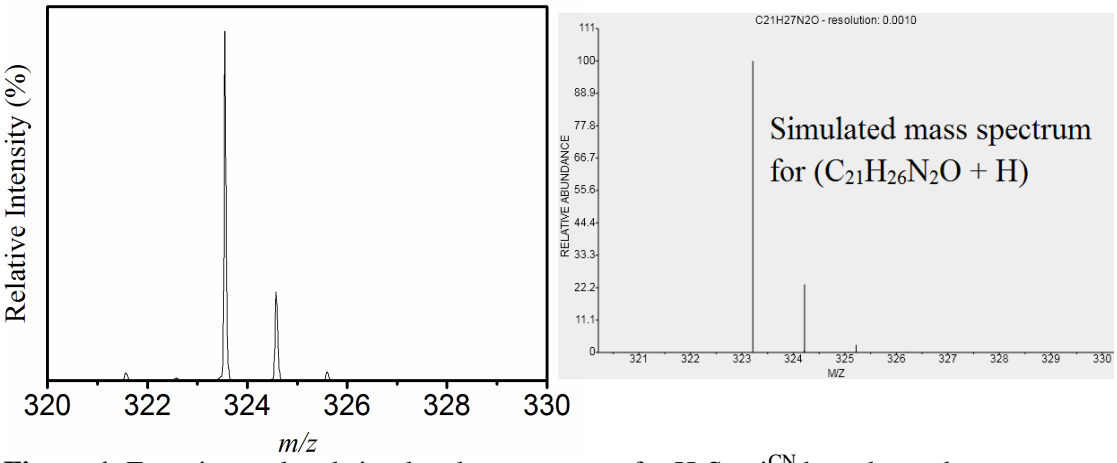

Figure 1. Experimental and simulated mass spectra for H_2Sami^{CN} have been shown.

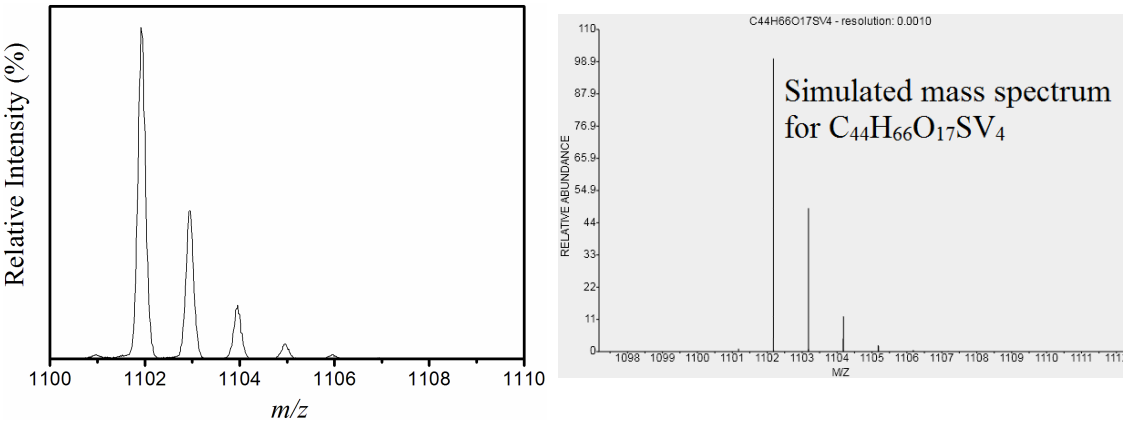

Figure 2. Experimental and simulated mass spectra for $[C_{44}H_{66}O_{17}SV_4]$ (the anionic cluster) have been shown.

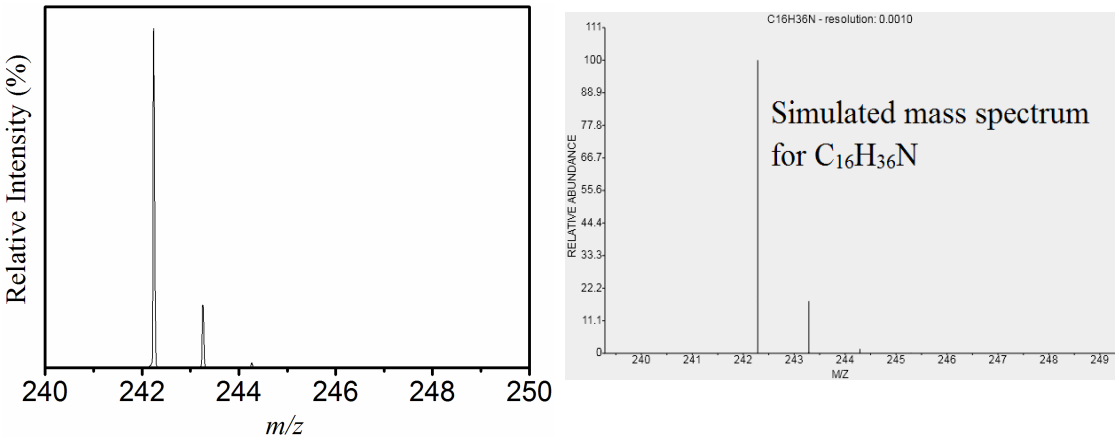

Figure 3. Experimental and simulated mass spectra for $[C_{16}H_{36}N]$ (tetrabutyl ammonium cation) have been shown.

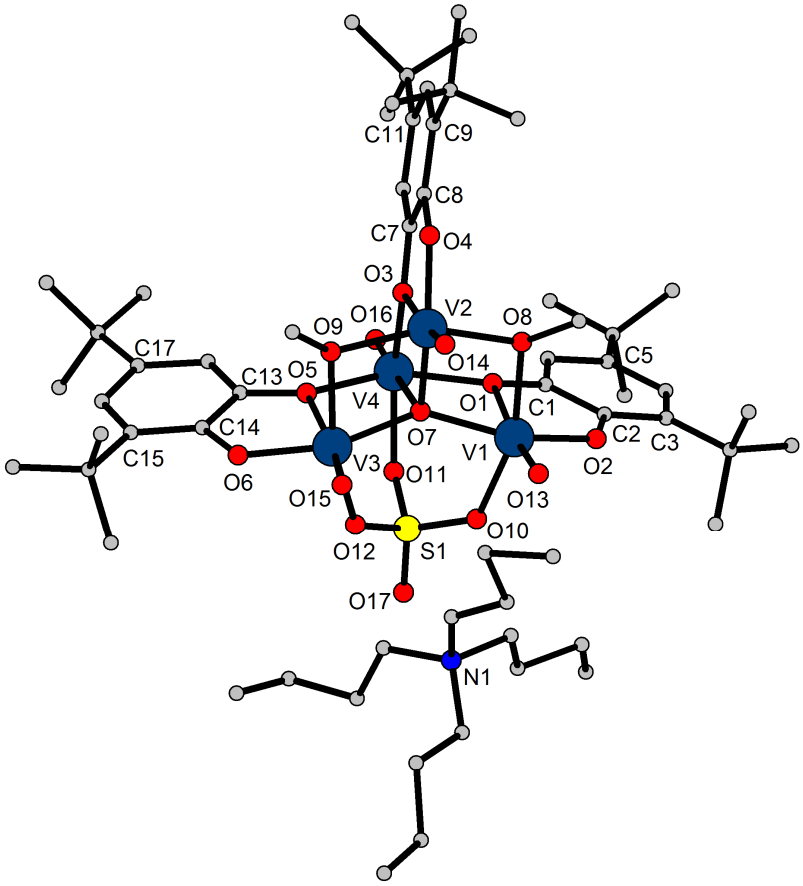

Figure 4. Molecular structure of **1** is shown. Solvent molecule CH_3CN and hydrogen atoms are omitted for clarity. A disorderness has been found in the tetrabutyl ammonium cationic part of the molecule.

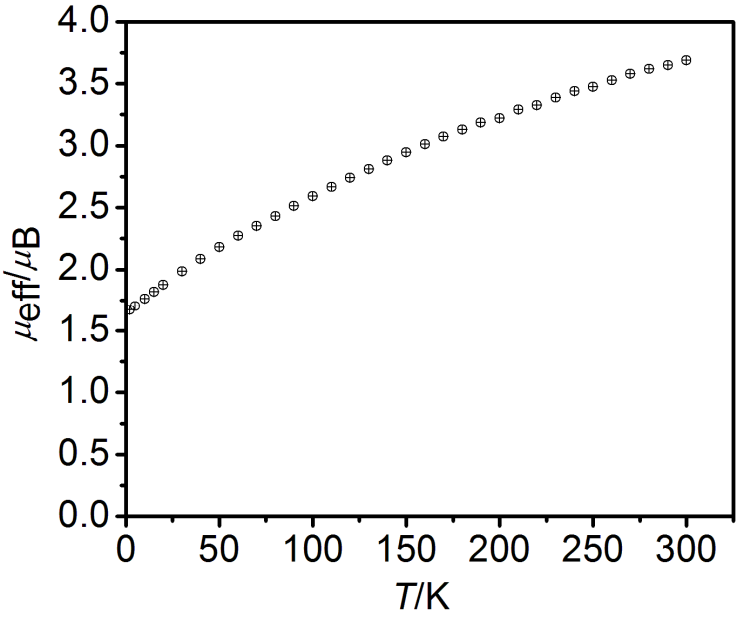

Figure 5. μ_{eff} vs T plot for **1**; B = 0.1T.

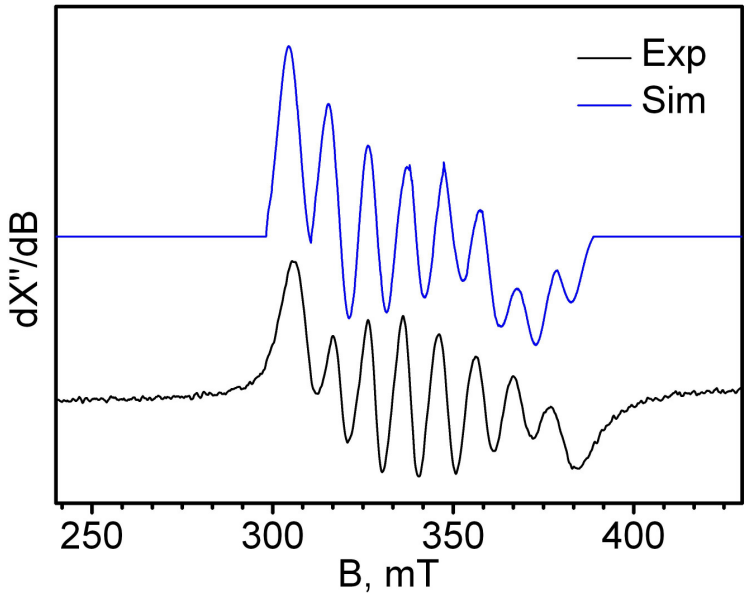

Figure 6. X-band EPR spectrum of complex **1** recorded at 25 °C in CH_2Cl_2 solution. Conditions: X-band microwave frequency (GHz), 9.451; modulation frequency (kHz), 100; modulation amplitude (G), 140.0; and microwave power, 0.998 [μW].

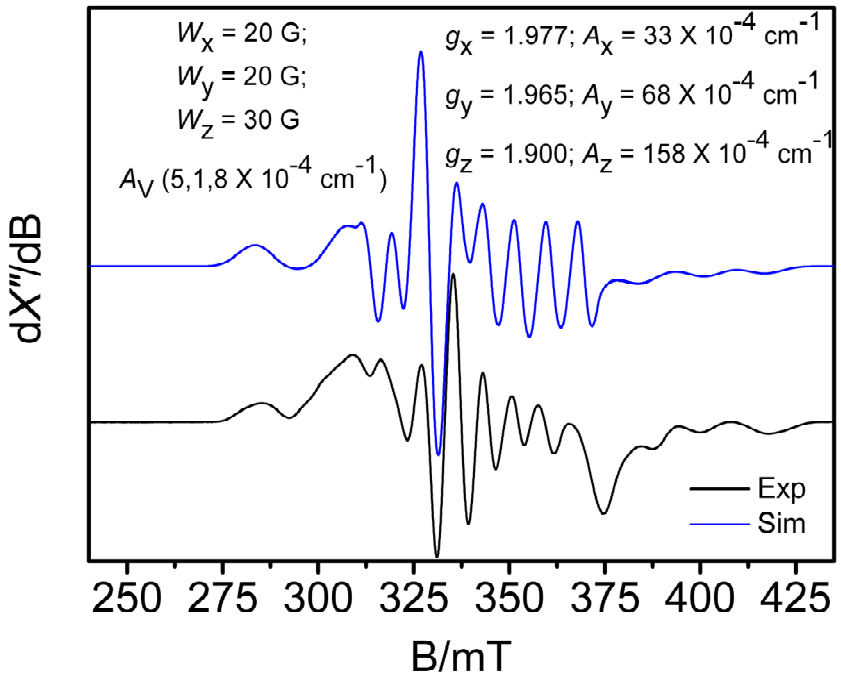

Figure 7. X-band EPR spectrum of complex **1** recorded at 25 °C in solid. Conditions: X-band microwave frequency (GHz), 9.450; modulation frequency (kHz), 100; modulation amplitude (G), 10.0; and microwave power, 0.998 [μW].

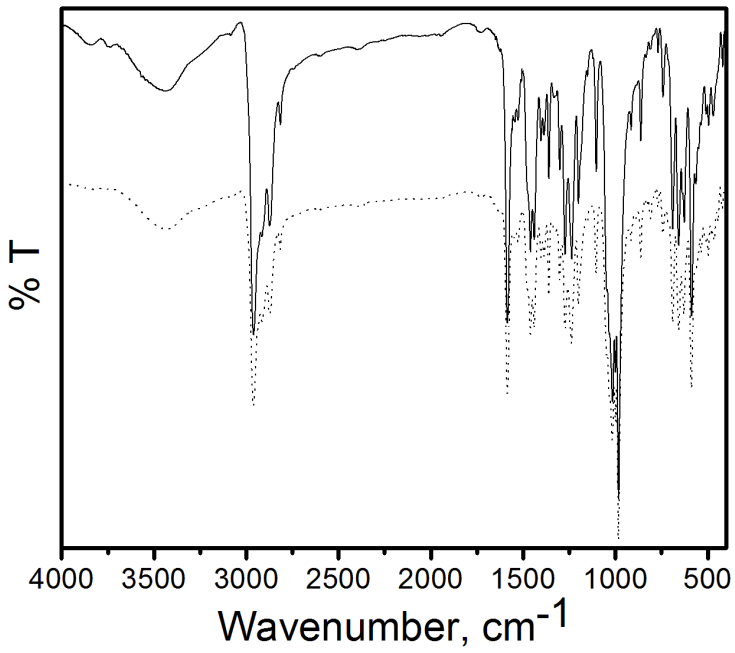

Figure 8. Infrared spectra of complex **1** (solid line) and **2** (dotted line) were shown.

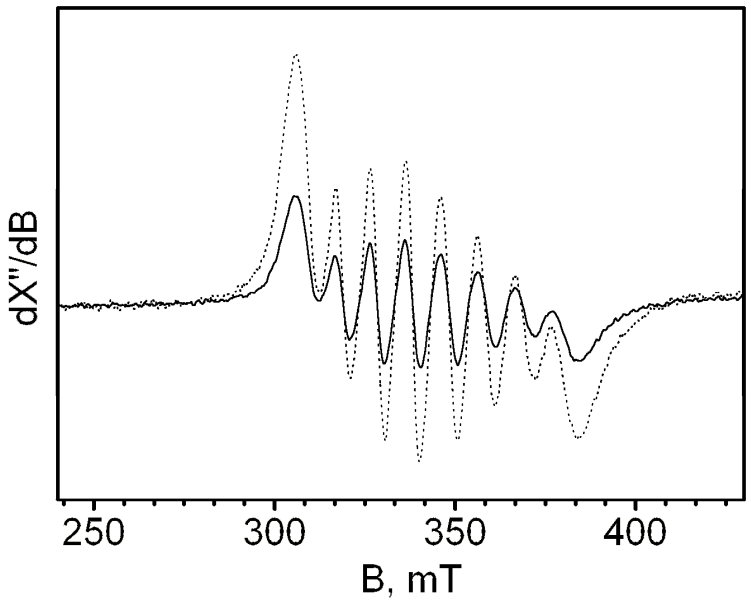

Figure 9. X-band EPR spectra of complex **1** (solid line) and **2** (dotted line) recorded at 25 °C in CH_2Cl_2 solution. Conditions: X-band microwave frequency (GHz), 9.451 (**1**), 9.452 (**2**); modulation frequency (kHz), 100 [**1** & **2**]; modulation amplitude (G), 140.0 [**1**], 300.0 [**2**]; and microwave power, 0.998 [μW] [**1** & **2**].

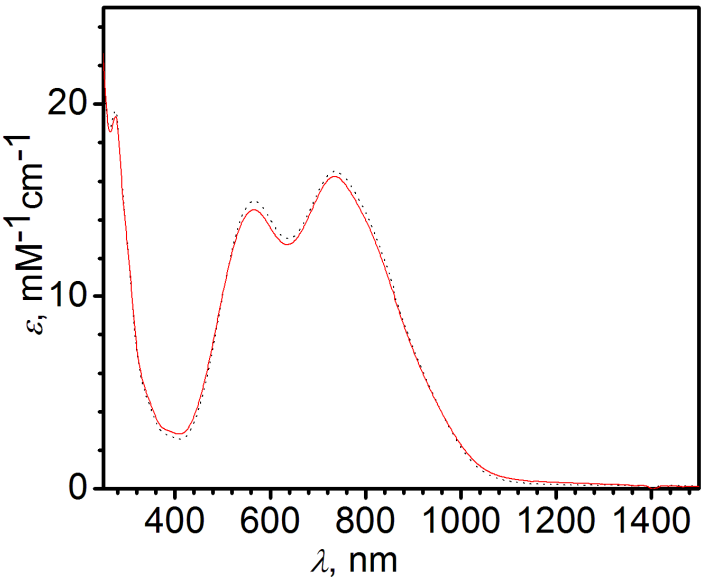

Figure 10. UV-vis/NIR spectra of complex **1** (solid line), and 2 (dotted line) measured at 25 °C in CH_2Cl_2 solution in 250-1500 nm range.

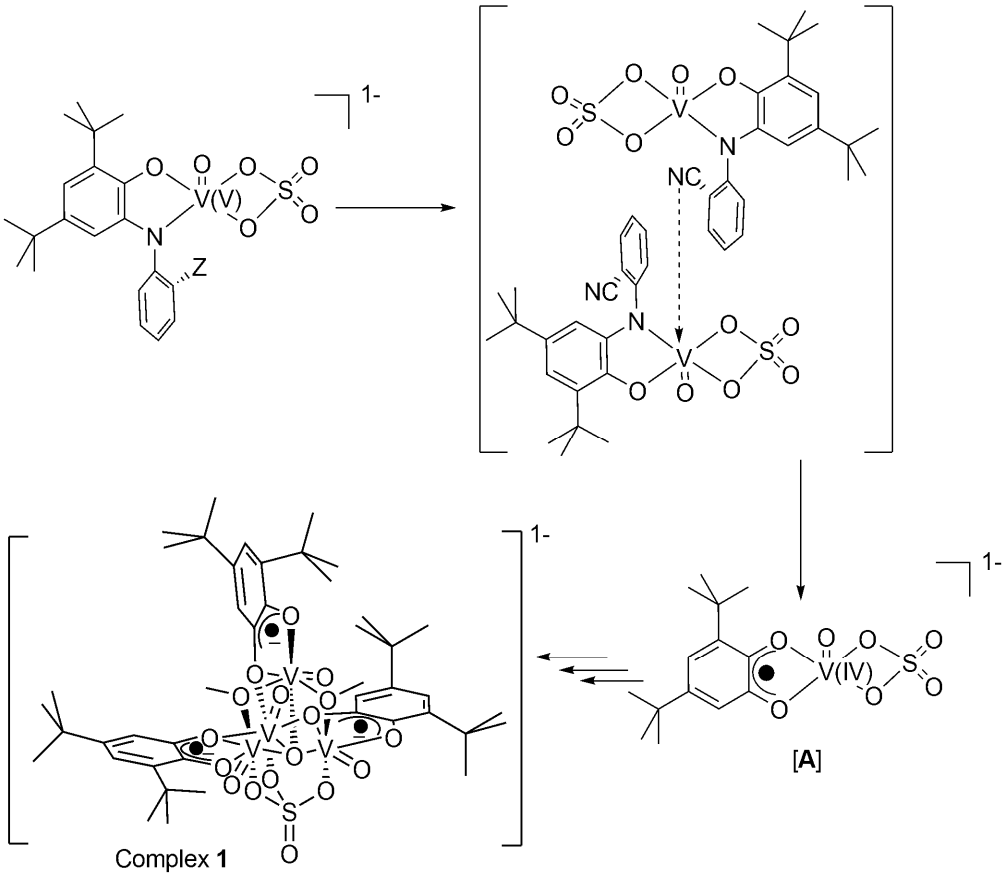

Figure 11. Showing the complex formed initially by the ligation of deprotonated ligand, SO_4^{2-} to vanadyl moiety. The proposed intermolecular weak interaction owing ambident and/or weak–coordination character by Z (–CN, –OMe). Intermediate [**A**] formed in the complex formation reaction using both ligands.

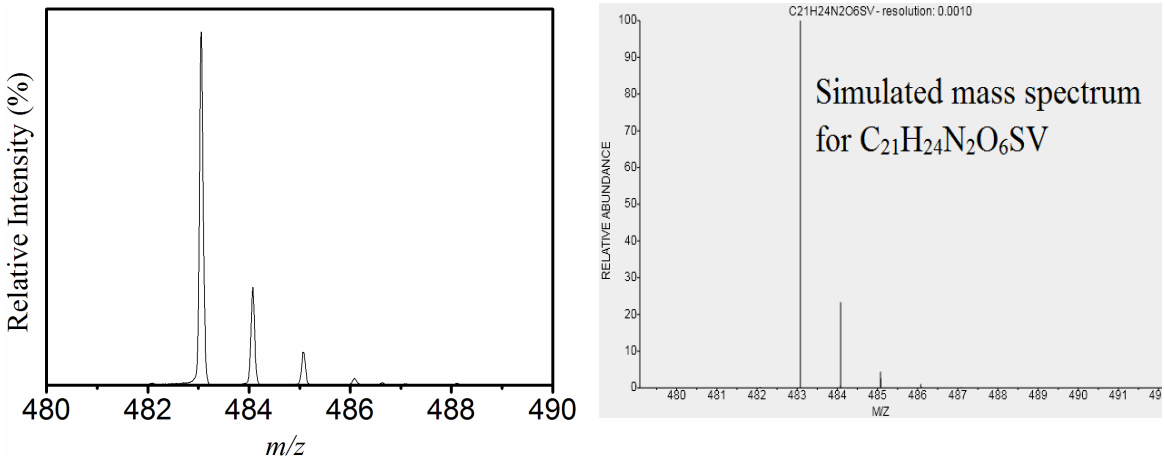

Figure 11a. Experimental and simulated mass spectra appeared in ESI–MS negative mode. Showing the complex formed initially by the ligation of deprotonated ligand, SO_4^{2-} to vanadyl moiety {[$C_{21}H_{24}N_2O_6SV$], (Z = –CN)} have been shown.

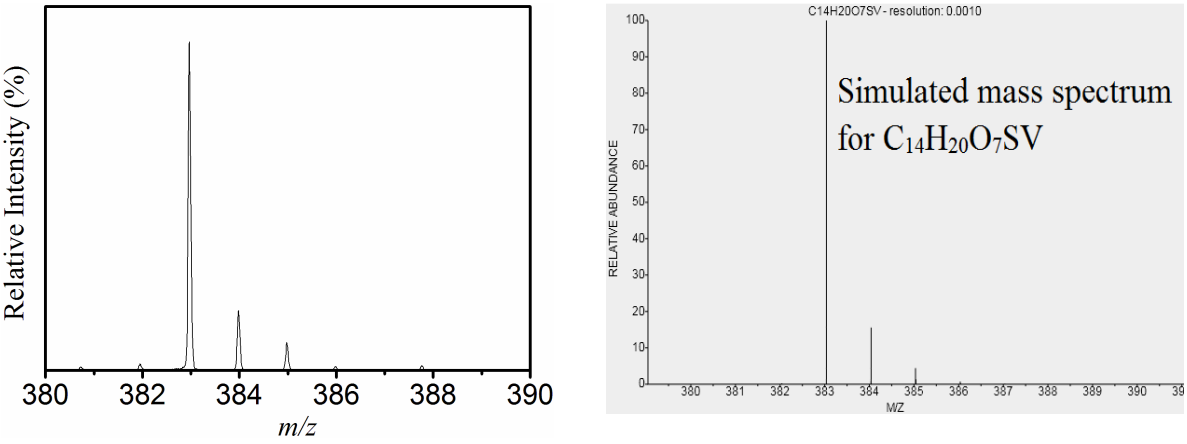

Figure 11b. Experimental and simulated mass spectra (ESI–MS negative mode) for [$C_{21}H_{20}O_7SV$] ([**A**]) species formed during the complex formation reaction.

Table 1. Crystallographic data and structure refinement for **1**, [$C_{60}H_{102}N_1O_{17}SV_4$•1$CH_3CN$].

Empirical formula	$C_{60}H_{102}N_1O_{17}SV_4$•1$CH_3CN$
Formula weight	1386.30
Crystal habit, colour	block, blue
Crystal size, mm	0.43 X 0.32 X 0.24
Temperature, T / K	296(2)
Wavelength, λ /Å	0.71073
Crystal system	orthorhombic
Space group	P b c a
Unit cell dimensions/Å	a = 25.3631(9) b = 20.7112(7) c = 28.6263(9)
Volume, V/Å^3	15037.4(9)
Z	8
Calculated density/Mg•m^{-3}	1.225
Absorption coefficient, μ/mm^{-1}	0.569
F(000)	5880
θ range for data collection	1.46 to 25.00°
Limiting indices	$-30 \le h \le 30$, $-24 \le k \le 24$, $-34 \le l \le 34$
Reflection collected / unique	167729 / 13231 [R(int) = 0.0924]
Completeness to θ	99.90% (θ = 25.00°)
Max. and min. transmission	0.804 / 0.872
Refinement method	'SHELXL-97 (Sheldrick, 1997)'
Data / restraints / parameters	13231 / 5 / 799
Goodness–of–fit on F^2	1.014
Final R indices [I>2sigma(I)]	R1 = 0.0605, wR2 = 0.1453
R indices (all data)	R1 = 0.1065, wR2 = 0.1698
Largest diff. peak and hole	0.654 and –0.372 e·Å^{-3}

Table 2. Selected bond distances (Å) for **1**, [$C_{60}H_{102}N_1O_{17}SV_4$•1$CH_3CN$].

C1–C2	1.424(6)	C7–C8	1.410(6)	C13–C14	1.412(6)
C2–C3	1.414(6)	C8–C9	1.406(6)	C14–C15	1.417(6)
C3–C4	1.371(6)	C9–C10	1.388(6)	C15–C16	1.377(6)
C4–C5	1.421(6)	C10–C11	1.407(6)	C16–C17	1.407(6)
C5–C6	1.381(7)	C11–C12	1.393(6)	C17–C18	1.388(6)
C6–C1	1.395(6)	C12–C7	1.376(6)	C18–C13	1.387(6)
V1–O1	2.242(3)	V2–O3	2.244(3)	V3–O5	2.236(3)
V1–O2	1.862(3)	V2–O4	1.839(3)	V3–O6	1.872(3)
V1–O7	1.937(3)	V2–O7	1.964(3)	V3–O7	1.946(3)
V1–O8	1.987(3)	V2–O8	1.992(3)	V3–O9	1.992(3)
V1–O10	2.015(3)	V2–O9	1.969(3)	V3–O12	2.022(3)
V1–O13	1.583(3)	V2–O14	1.584(3)	V3–O15	1.584(3)
V4–O1	1.968(3)	C1–O1	1.316(5)	V1–V2	3.041(1)
V4–O3	1.983(3)	C2–O2	1.322(5)	V1–V3	3.672(1)
V4–O5	1.968(3)	C7–O3	1.333(5)	V1–V4	3.364(1)
V4–O7	2.408(3)	C8–O4	1.346(5)	V2–V3	3.040(1)
V4–O11	2.037(3)	C13–O5	1.329(5)	V2–V4	3.464(1)
V4–O16	1.577(3)	C14–O6	1.331(5)	V3–V4	3.364(1)
S1–O10	1.505(3)	S1–O12	1.506(3)		
S1–O11	1.499(3)	S1–O17	1.429(4)		

Table 3. Selected bond angles (°) for **1**, $[C_{60}H_{102}N_1O_{17}SV_4 \bullet 1CH_3CN]$.

C1–C2–O2	115.01(36)	C7–C8–O4	115.40(34)
C1–O1–V1	111.20(23)	C7–O3–V2	111.10(22)
C2–O2–V1	124.19(26)	C8–O4–V2	124.00(24)
C2–C1–O1	114.16(36)	C8–C7–O3	113.47(34)
O1–V1–O2	75.23(11)	O3–V2–O4	75.46(10)
O1–V1–O7	77.92(10)	O3–V2–O7	74.92(10)
O1–V1–O8	80.3(1)	O3–V2–O8	86.21(10)
O1–V1–O10	84.90(11)	O3–V2–O9	85.96(11)
O1–V1–O13	173.25(12)	O3–V2–O14	173.06(12)
O2–V1–O7	153.09(12)	O4–V2–O7	150.14(12)
O2–V1–O8	96.38(12)	O4–V2–O8	97.76(12)
O2–V1–O10	93.98(12)	O4–V2–O9	104.58(13)
O2–V1–O13	98.44(14)	O4–V2–O14	97.62(14)
O7–V1–O8	77.36(11)	O7–V2–O8	76.65(11)
O7–V1–O10	85.21(11)	O7–V2–O9	76.97(11)
O7–V1–O13	108.32(13)	O7–V2–O14	112.02(14)
O8–V1–O10	159.11(12)	O8–V2–O9	153.60(13)
O8–V1–O13	98.32(13)	O8–V2–O14	95.33(14)
O10–V1–O13	98.03(13)	O9–V2–O14	95.47(14)
V1–O1–V4	105.89(11)	V2–O3–V4	109.91(12)
C13–C14–O6	115.94(36)	O1–V4–O3	88.87(11)
C13–O5–V3	111.44(23)	O1–V4–O5	145.58(11)
C14–O6–V3	123.24(26)	O1–V4–O7	73.36(10)
C14–C13–O5	113.83(35)	O1–V4–O11	83.93(11)
O5–V3–O6	75.47(11)	O1–V4–O16	107.42(13)
O5–V3–O7	77.96(10)	O3–V4–O5	88.68(11)
O5–V3–O9	80.41(11)	O3–V4–O7	70.83(10)
O5–V3–O12	84.59(11)	O3–V4–O11	155.37(11)
O5–V3–O15	173.67(13)	O3–V4–O16	104.57(13)
O6–V3–O7	153.23(13)	O5–V4–O7	73.43(10)
O6–V3–O9	95.47(13)	O5–V4–O11	84.19(12)
O6–V3–O12	95.95(13)	O5–V4–O16	106.41(13)
O6–V3–O15	98.27(14)	O7–V4–O11	84.54(10)
O7–V3–O9	76.82(11)	O7–V4–O16	175.38(12)
O7–V3–O12	84.69(12)	O11–V4–O16	100.05(13)
O7–V3–O15	108.23(13)	V1–O7–V2	102.43(12)
O9–V3–O12	158.22(13)	V1–O7–V3	141.99(15)
O9–V3–O15	99.47(14)	V1–O7–V4	100.88(11)
O12–V3–O15	97.16(15)	V2–O7–V3	102.10(12)
V3–O5–V4	106.09(12)	V2–O7–V4	104.34(11)
		V3–O7–V4	100.62(11)